Optimal filter characterization for photoplethysmography-based pulse rate and pulse power spectrum estimation

Raymundo Cassani, Abhishek Tiwari, and Tiago H. Falk

Abstract— **Photoplethysmography (PPG) is a non-invasive, low-cost optical technique used to assess the cardiovascular system. In recent years, PPG-based heart rate measurement has gained significant attention due to its popularity in wearable devices, as well as its practicality relative to electrocardiography (ECG). Studies comparing the dynamics of ECG- and PPG-based heart rate measures have found small differences between these two modalities; differences related to the physiological processes behind each technique. In this work, we analyzed the spectral coherence and the signal-to-noise ratio between isolated PPG pulses and the raw PPG signal in order to: (i) determine the optimal filter to enhance pulse detection from raw PPG for improved heart rate estimation, and (ii) characterize the spectral content of the PPG pulse. The proposed methods were evaluated on 27000 pulses from a PPG database acquired from 42 participants (adults and children). The results showed that the optimal bandpass filter to enhance PPG from the adult group was 0.6-3.3 Hz, while for the children group it was 1.0-2.7 Hz. The spectral analysis on the pulse signal showed that similar bandwidths were found for the adult (0.8-2.4 Hz) and children (0.9-2.7 Hz) groups. We hope that the results presented herein serve as a baseline for pulse detection algorithms and assist with the development of more sophisticated PPG processing algorithms.**

I. Introduction

Photoplethysmography (PPG) is a non-invasive, low-cost optical technique that detects the pulsatile changes in blood volume. A PPG device is comprised of two main components: a light source that sheds light on the skin and a detector that measures small variations in the intensity of the back-scattered light. These variations are related to the changes in blood volume that occur with each cardiac pulse. Despite the fact that the specific origins of the PPG signal are not completely understood, its importance for the assessment of the cardiovascular system is widely accepted. Some PPG clinical applications include: pulse oximetry, assessment of arterial stiffness, study of hypertension, estimation of heart and respiration rates, among others [1], [2], [3], [4], [5], [6].

Traditionally, heart rate (HR) is derived from the electrocardiogram (ECG) signal. Given the fact that PPG measures the blood volume changes at each pulse, PPG can also be used to estimate the HR. To differentiate EEG-based HR and PPG-based HR, in this work, the first is referred to as HR, and the later as pulse rate (PR). Besides the importance of HR as a vital sign, the analysis of its variability (HRV) has been shown useful to assess the cardiovascular system, to monitor the autonomic nervous system, and for human factors analysis, such as fatigue, mental workload, and anxiety measurement, to name a few [7], [8], [9].

Compared with ECG, PPG is a more convenient measurement technique as it does not require electrodes and can be measured from peripheral locations, such as fingertip, ear, or toes. This has resulted in a popular demand for PPG in wearable devices. To this end, several works have evaluated the PR variability (PRV) as a correlate (or surrogate) of ECG-based HRV. Studies comparing HRV and PRV with subjects at rest have found high correlation both in terms of features [4], [10], [11], as well as power spectra [12]. Notwithstanding, these correlations have shown to diminish when HRV and PRV are compared after exercise, in subjects with cardiovascular diseases [13], or during physical activity and mental stress [12], [4]. It has been reported that these differences between PRV and HRV are due to differences in the underlying physiological processes, rather than only in an inaccurate pulse location [4]. While PRV can not be regarded as a substitute for HRV, its analysis can provide relevant (and potentially complementary) information about the subject. In [9], for example, the analysis of PRV was used for the estimation of stress and anxiety in nurses.

An accurate estimation of the PR (and PRV) can be difficult as the PPG signal is often corrupted by noise from different sources, such as sensor movement and displacement. To compute PR, the raw PPG signal is first low-pass filtered to reduce artifacts and high-pass filtered to remove the DC component. However, the cutoff frequencies of these filters vary from study to study, being 0.5 Hz a common selection for the high-pass filter, while common cutoff frequency values for the low-pass filter range from 2 to 15 Hz, based on the spectral content of the PPG signal [14]. In the PPG literature, few works have searched for the best filter configuration. In [15], for example, the best filter for pulse oximetry was discussed. In [16], in turn, the best filter to improve PPG kurtosis (a quality metric) was found. However, to the best of our knowledge, no study exists that search for an optimal filter to improve pulse detection in the PPG signal. This work aims to fill this gap.

More specifically, the main goal of this work is to find the optimal filter to process raw PPG signals, in order to preserve the spectral content that is relevant for the detection of the pulse and, ultimately, for PR and PRV measurement. The approach taken here is similar to the one presented in [17] for ECG. Moreover, a secondary goal of this work is to determine the spectral content of the PPG pulse, as such information can serve as stepping stone for the development of more sophisticated pulse detection algorithms.

Authors are with the Institut National de la Recherche Scientifique (INRS-EMT), University of Quebec, Montreal, QC, Canada. raymundo.cassani@emt.inrs.ca

978-1-7281-1990-8/20/$31.00 ©2020 IEEE

II. Methods and Materials

A. Dataset

Data used in this study corresponds to the PPG recordings and pulse-peak locations of the "Capnobase IEEE TBME Respiratory Rate Benchmark dataset" [6]. This dataset contains forty-two 8-minute PPG recordings, obtained from two groups, 13 adults (age: 47.2 ± 9.3 years) and 29 children (age: 8.7 ± 5.4 years). The PPG signals were acquired with a sampling frequency of 300 Hz using the fingertip Phone Oximeter [18]. The pulse peak and artifact labels have been validated by an expert rater.

B. Methods

For an accurate estimation of the PR, the component of main interest of the PPG signal is the pulse (and its peak location). Based on this, the PPG signal, $y(t)$, can be modeled as the pulse signal, $x(t)$ convolved with a system with impulse response $h(t)$ and with additive noise $n(t)$:

$$y(t) = h(t) * x(t) + n(t), \tag{1}$$

or in the frequency domain as:

$$Y(f) = H(F)X(f) + N(f), \tag{2}$$

with $Y(f)$, $X(f)$ and $N(f)$ being the spectra for the $y(t)$, $x(t)$ and $n(t)$ signals respectively, and $H(f)$ is the frequency response of the system.

Magnitude square coherence, $C^2_{xy}(f)$, frequently referred to just as "coherence" is a measure of co-variance between two power spectra, i.e., it can be used to explore the power relation between the input and the output of a system, and is defined as follows:

$$C^2_{xy}(f) = \frac{|S_{yx}(f)|^2}{S_{yy}(f)S_{xx}(f)}, \tag{3}$$

where $S_{yx}(f)$ is the cross-spectrum for the signals $y(t)$ and $x(t)$; and $S_{yy}(f)$ and $S_{xx}(f)$ are their respective auto-spectra or power spectral densities. These terms are defined below, where all terms are functions of frequency, but this is not explicitly shown for sake of simplicity.

$$S_{xx} = XX^* = |X|^2, \tag{4}$$

$$\begin{aligned} S_{yy} &= YY^* = (HX + N)(HX + N)^* \\ &= |H|^2 S_{xx} + HS_{xn} + H^* S_{nx} + S_{nn}, \end{aligned} \tag{5}$$

$$S_{yx} = YX^* = (HX + N)(X)^* = HS_{xx} + S_{xn}. \tag{6}$$

The cross-spectrum $S_{yx}(f)$ is an indication of how common activity of the individual signals is at each frequency component. Thus, $|S_{yx}(f)|^2$ is the cross-power between the signals. Moreover, assuming that $x(t)$ and $n(t)$ are uncorrelated signals, then $S_{xn} = S_{nx} = 0$. As such, (3) can be rewritten as:

$$\begin{aligned} C^2_{xy} &= \frac{(HS_{xx})(HS_{xx})^*}{S_{xx}(|H|^2 S_{xx} + S_{nn})} \\ &= \frac{|H|^2 S_{xx}}{|H|^2 S_{xx} + S_{nn}} = \frac{|H|^2 S_{xx}}{S_{yy}}. \end{aligned} \tag{7}$$

In this sense, (7) can be seen as the ratio of coherent power (power due to the signal $x(t)$) to the total power, i.e., the sum of coherent power and non-coherent power (noise). Thus, $1 - C^2_{xy}$ is the ratio of non-coherent power to total power. Therefore, the signal-to-noise ratio (SNR) is defined as:

$$SNR(f) = \frac{C^2_{xy}(f)}{1 - C^2_{xy}(f)} = \frac{|H(f)|^2 S_{xx}(f)}{S_{nn}(f)}. \tag{8}$$

Finally, we define the optimal filter to enhance the PPG signal for PR estimation as the one that maximizes this SNR.

C. Processing

For each pulse peak location in the dataset, two PPG signal segments with center in the pulse peak location were obtained. First a 1.7 s segment of the PPG signal, and a 1 s segment for the pulse signal; these signals constitute $y(t)$ and $x(t)$ in (1), respectively. The DC component was removed, and both signals were windowed with a Tukey window, as it provides a "flat top" to avoid significant attenuation of the signal [19]. With the use of the Tukey window ($\alpha = 0.8$) the PPG and pulse signals had an effective duration of 850 ms and 500 ms, respectively [20]. The pulse signal was zero padded before and after to have the same length as the PPG segment. These processing steps are depicted in Figure 1.

Subsequently, the estimations for $S_x x$, $S_y y$ and $S_y x$, i.e., $\hat{S}_x x$, $\hat{S}_y y$ and $\hat{S}_y x$ respectively, were calculated from the n pulse-peak locations that were processed as follows:

$$\hat{S}_{xx} = \frac{1}{n}\sum_{i=1}^{n} X_n X_n^*,$$

$$\hat{S}_{yy} = \frac{1}{n}\sum_{i=1}^{n} Y_n Y_n^*,$$

$$\hat{S}_{yx} = \frac{1}{n}\sum_{i=1}^{n} X_n Y_n^*.$$

With these estimators, the coherence and SNR are computed with (3) and (8), respectively. Finally, the bandwidth (BW) of the optimal filter is defined as the bandwidth of the SNR function up to 6 dB below the maximum SNR value.

III. Results

In total, over 27,000 pulses were processed. From these pulses, around 27% came from the adult group. The PPG and pulse signals were separately processed for each of the two groups, and the average signals are presented in Figure 2. Coherence and SNR frequency functions, as well as the optimal filter to enhance PR estimation are depicted for both groups in Figure 3. The optimal filter derived form the recordings in the adult group had a lower cutoff frequency, f_{c1}, of 0.6 Hz and a upper cutoff frequency, f_{c2}, of 3.3 Hz. In turn, the optimal filter from the children group had a f_{c1} of 1.0 Hz and f_{c2} of 2.7 Hz. Additionally, the BW of the pulse signal was obtained by measuring its half-power BW, resulting in a BW of 0.8 Hz to 2.4 Hz for the adult group, and 0.9 Hz to 2.7 Hz for the children group.

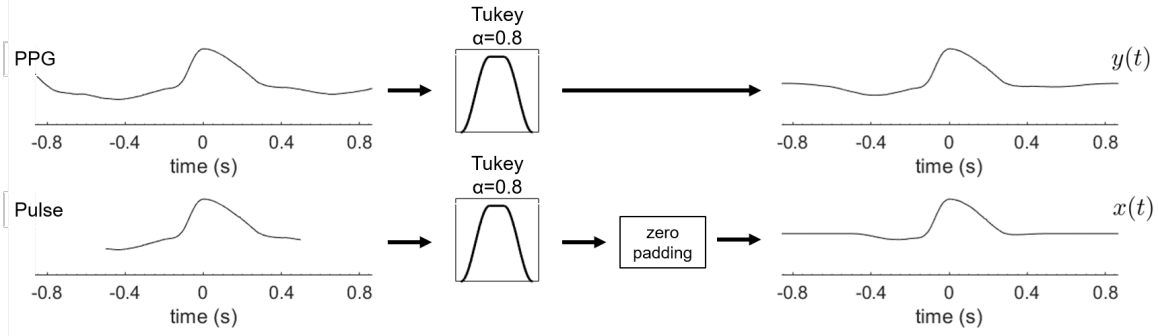

Fig. 1. Processing steps performed on the PPG and the pulse signals.

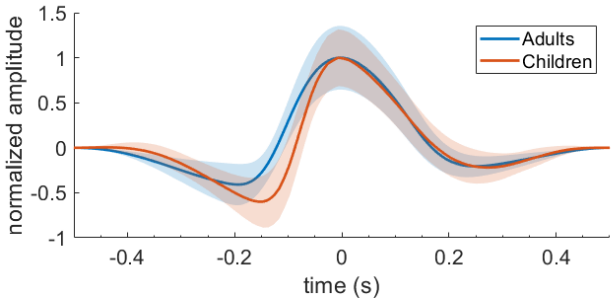

Fig. 2. Average pulse signals for both groups: adults (blue) and children (red). Signals have been scaled for sake of comparison, and the shadowed area presents one standard deviation.

Additionally, we merged the data from the four participants in the children's dataset who were older than 16 years (thus leading to a total of 17 participants) to compute a more general depiction of the PPG pulse. The derived coherence and SNR functions are depicted in Figure 4, where the optimal filter had a f_{c1} of 0.6 Hz and a f_{c2} of 3.3 Hz. The BW of the pulse signal for this group was 0.9 Hz to 2.6 Hz.

With these insights, Figure 5 depicts a segment of a raw PPG signal along with its corresponding signal filtered with the proposed optimal filter (bandpass from 0.6 to 3.3 Hz) implemented as an IIR Butterworth filter of second order.

IV. Discussion

Morphological differences in the pulse signal obtained from the adult and children groups are shown in Figure 2. These differences include a deeper pulse foot and a steeper slope in the rising edge for the children group; while the adult population presented a slightly wider pulse. In the literature, such age-related changes in pulse characteristics have been reported, such as longer delay between systolic and diastolic peaks, and smoother pulse shape with age, both due to an increase in artery stiffens [21], [22], [23], [24].

The proposed optimal filter can be implemented in diverse manners, however, it is important to keep a relatively short time constant to avoid interference with the previous processed pulse. As such, IIR filters are preferable to FIR filters for this application, as the latter require a large number of taps to obtain the same frequency response. It is worth noting that the optimal-filter BW resembles the pulse BW for the groups under analysis.

Lastly, the optimal filter and the pulse BW obtained in this work were based on PPG signals from the fingertip, which is the most popular recording location. Nevertheless, in the last years wrist PPG has gained traction with the appearance of heart-rate monitors and smartwatches. In recent works, fingertip and wrist PPG have been compared in terms of morphology [25] and their usability to calculate the pulse arrival time [26]. Given the reported differences, the filter found here may not be optimal for wrist PPG. As such, an extension for the present work would be to perform the analysis on pulses from wrist-measured PPG. A limitation in this work was the small size of the adult sample (N=13). We expect that future works will analyze this methodology with larger samples. For this purpose, the codes used in this work are available at: https://github.com/rcassani/PPG-pulse-bw

V. Conclusions

Filtering is a pivotal step in the processing of PPG signal. It removes the DC component and rejects undesired signals and artifacts. Across the PPG literature, however, there is no consensus on the cutoff frequencies the filters, with varying values being reported for different studies. In this work, we developed an optimal filter for the computation of PR from raw PPG using insights obtained from over 27000 PPG pulses, thus providing the research community with a baseline method for PPG/PR/PRV comparisons. Moreover, an estimation of the power spectrum of the pulse component of the PPG signal is provided, thus complementing the existing PPG literature.

References

[1] A. V. Moço, S. Stuijk, and G. de Haan, "New insights into the origin of remote PPG signals in visible light and infrared," *Scientific Reports*, vol. 8, no. 1, p. 8501, Dec. 2018.

[2] J. Allen, "Photoplethysmography and its application in clinical physiological measurement," *Physiological Measurement*, vol. 28, no. 3, pp. R1–R39, Mar. 2007.

[3] D. Castaneda, A. Esparza, M. Ghamari, C. Soltanpur, and H. Nazeran, "A review on wearable photoplethysmography sensors and their potential future applications in health care," *International journal of biosensors & bioelectronics*, vol. 4, no. 4, p. 195, 2018.

[4] A. Schäfer and J. Vagedes, "How accurate is pulse rate variability as an estimate of heart rate variability?" *International Journal of Cardiology*, vol. 166, no. 1, pp. 15–29, Jun. 2013.

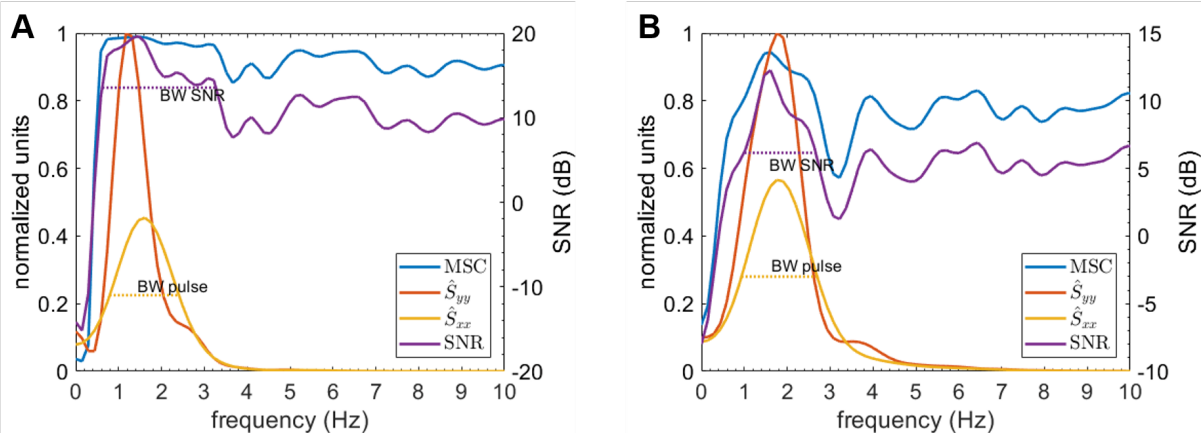

Fig. 3. Power spectra, coherence and SNR for: (A) Adult, and (B) Children. Dotted lines indicate the BW of the optimal filter, and the pulse signal.

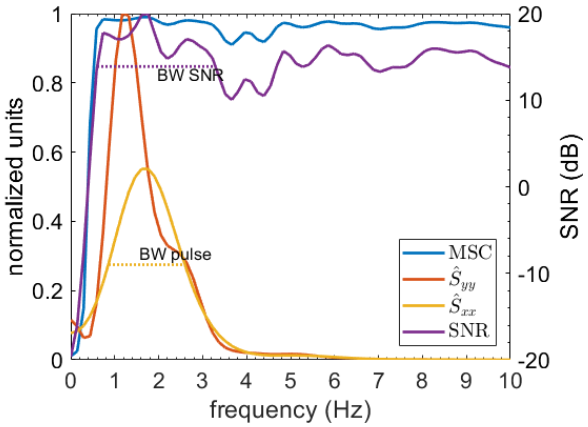

Fig. 4. Power spectra, coherence and SNR for participants older than 16 years. Dotted lines indicate the BW of the optimal filter, and the pulse signal.

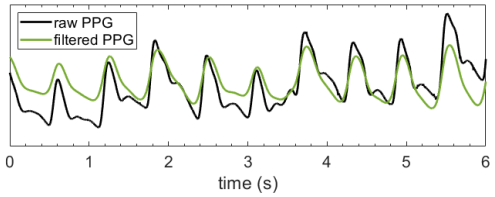

Fig. 5. Raw and filtered PPG.

[5] M. Elgendi, R. Fletcher, Y. Liang, N. Howard, N. H. Lovell, D. Abbott, K. Lim, and R. Ward, "The use of photoplethysmography for assessing hypertension," *npj Digital Medicine*, vol. 2, no. 1, p. 60, Dec. 2019.

[6] W. Karlen, S. Raman, J. M. Ansermino, and G. A. Dumont, "Multiparameter Respiratory Rate Estimation From the Photoplethysmogram," *IEEE Trans Biomedical Eng*, vol. 60, no. 7, pp. 1946–1953, Jul. 2013.

[7] Task Force of the European Society of Cardiology the North American Society of Pacing, "Heart Rate Variability," *Circulation*, vol. 93, no. 5, pp. 1043–1065, Mar. 1996.

[8] P. Stein and R. Kleiger, "Insights from the study of heart rate variability," *Annual Review Medicine*, vol. 50, no. 1, pp. 249–261, 1999.

[9] A. Tiwari, R. Cassani, S. Narayanan, and T. H. Falk, "A Comparative Study of Stress and Anxiety Estimation in Ecological Settings Using a Smart-shirt and a Smart-bracelet," in *IEEE EMBC*, 2019, pp. 2213–2216.

[10] V. Jeyhani, S. Mahdiani, M. Peltokangas, and A. Vehkaoja, "Comparison of HRV parameters derived from photoplethysmography and electrocardiography signals," in *IEEE EMBC*, 2015, pp. 5952–5955.

[11] S. Lu, H. Zhao, K. Ju, K. Shin, M. Lee, K. Shelley, and K. H. Chon, "Can Photoplethysmography Variability Serve as an Alternative Approach to Obtain Heart Rate Variability Information?" *J Clinical Monitoring and Computing*, vol. 22, no. 1, pp. 23–29, Jan. 2008.

[12] W.-H. Lin, D. Wu, C. Li, H. Zhang, and Y.-T. Zhang, "Comparison of Heart Rate Variability from PPG with That from ECG," in *Intl Conf Health Informatics*, Y.-T. Zhang, Ed., 2014, vol. 42, pp. 213–215.

[13] N. Pinheiro, R. Couceiro, J. Henriques, J. Muehlsteff, I. Quintal, L. Goncalves, and P. Carvalho, "Can PPG be used for HRV analysis?" in *IEEE EMBC*, 2016, pp. 2945–2949.

[14] A. Kamal, J. Harness, G. Irving, and A. Mearns, "Skin photoplethysmography—a review," *Computer methods and programs in biomedicine*, vol. 28, no. 4, pp. 257–269, 1989.

[15] N. Stuban and M. Niwayama, "Optimal filter bandwidth for pulse oximetry," *Review Scientific Inst*, vol. 83, no. 10, p. 104708, 2012.

[16] Y. Liang, M. Elgendi, Z. Chen, and R. Ward, "An optimal filter for short photoplethysmogram signals," *Scientific Data*, vol. 5, no. 1, p. 180076, Dec. 2018.

[17] N. V. Thakor, J. G. Webster, and W. J. Tompkins, "Optimal QRS detector," *Medical & Biological Engineering & Computing*, vol. 21, no. 3, pp. 343–350, May 1983.

[18] W. Karlen, G. A. Dumont, C. Petersen, J. Gow, J. Lim, J. Sleiman, and J. M. Ansermino, "Human-centered phone oximeter interface design for the operating room," in *International Conference on Health Informatics*, 2011, pp. 433–438.

[19] F. Harris, "On the use of windows for harmonic analysis with the discrete Fourier transform," *Proceedings of the IEEE*, vol. 66, no. 1, pp. 51–83, 1978.

[20] R. Cassani and T. H. Falk, "Spectrotemporal Modeling of Biomedical Signals: Theoretical Foundation and Applications," in *Reference Module in Biomedical Sciences*. Elsevier, 2018.

[21] S. Millasseau, R. Kelly, J. Ritter, and P. Chowienczyk, "Determination of age-related increases in large artery stiffness by digital pulse contour analysis," *Clinical Science*, vol. 103, no. 4, pp. 371–377, Oct. 2002.

[22] M. Elgendi, "On the Analysis of Fingertip Photoplethysmogram Signals," *Current Cardiol Reviews*, vol. 8, no. 1, pp. 14–25, 2012.

[23] J. Allen and A. Murray, "Age-related changes in the characteristics of the photoplethysmographic pulse shape at various body sites," *Physiological Measurement*, vol. 24, no. 2, pp. 297–307, May 2003.

[24] M. F. O'Rourke, A. Pauca, and X.-J. Jiang, "Pulse wave analysis," *British J Clinical Pharmacology*, vol. 51, no. 6, pp. 507–522, 2001.

[25] V. Hartmann, H. Liu, F. Chen, Q. Qiu, S. Hughes, and D. Zheng, "Quantitative Comparison of Photoplethysmographic Waveform Characteristics: Effect of Measurement Site," *Frontiers in Physiology*, vol. 10, p. 198, Mar. 2019.

[26] S. Rajala, H. Lindholm, and T. Taipalus, "Comparison of photoplethysmogram measured from wrist and finger and the effect of measurement location on pulse arrival time," *Physiological Measurement*, vol. 39, no. 7, p. 075010, Aug. 2018.